Indirect exchange interaction in two-dimensional materials with quartic dispersion

Ahmet Utku Canbolat [1,*] Hâldun Sevinçli [2] and Özgür Çakır [1,†]
[1]*Department of Physics, Izmir Institute of Technology, 35430 Urla, Izmir*
[2]*Department of Material Science and Engineering, Izmir Institute of Technology, 35430 Urla, Izmir*

(Received 17 August 2021; revised 1 August 2022; accepted 2 September 2022; published 12 September 2022)

We investigate the indirect magnetic exchange interaction between two magnetic moments in a two-dimensional semiconductor with quartic dispersion, featuring a singularity at the band edge. We obtain the Green's functions analytically to calculate the magnetic exchange interaction at zero temperature. We show that the singularity in the density of states (DOS) for quartic dispersion gives rise to an enhancement in the amplitude of the Ruderman-Kittel-Kasuya-Yosida (RKKY) interaction as the Fermi energy is swept toward the band edge. Furthermore, a region of finite exchange interaction arises, with a range increasing as the Fermi energy approaches the band edge. The results lay the possibility of an electrical/chemical control over the exchange interactions.

DOI: 10.1103/PhysRevB.106.104409

I. INTRODUCTION

Ruderman-Kittel-Kasuya-Yosida (RKKY) interaction is an indirect exchange interaction between localized magnetic moments mediated by conduction electrons [1–3]. In a d-dimensional metallic system with parabolic energy dispersion, RKKY interaction oscillates at the Fermi wavelength featuring ferromagnetic (FM) and antiferromagnetic (AF) character as a function of distance and it decays as $1/R^d$, for $d = 1, 2, 3$ [4,5]. In doped graphene the exchange interaction decays as $1/R^2$ oscillating at the Fermi wavelength between FM/AF values [6,7]. In neutral two-dimensional monolayer graphene the RKKY interaction decays as $1/R^3$, which arises due to vanishing DOS at the Fermi energy. In neutral graphene, exchange energy is of pure ferromagnetic (antiferromagnetic) character depending on whether the impurities are located at the same (different) sublattice of the hexagonal lattice [8–10]. The difference in chirality of valence and conduction electronic states and particle-hole symmetry in neutral graphene leads to a purely AF/FM-type magnetic interaction depending on the sublattice type of the impurities [8].

The importance of dispersion and the density of states (DOS) at the Fermi energy for two-dimensional materials was explored by Klier *et al.* [10], who reported a change in the range and AF/FM character of RKKY interactions in biased bilayer graphene as the Fermi energy is tuned across the band edge [11]. For graphene monolayers the enhancement of DOS at the Fermi level via resonances created by external potentials and its influence on RKKY interactions was explored in Ref. [12].

It was reported that group VA and group III-VI elements can form stable two-dimensional monolayer structures, exhibiting quartic dispersion where the quartic dispersion leads to a van Hove singularity in the DOS at the valence band edge [13–15]. At the valence band edge these materials feature a dispersion of the form $E = -\alpha(k^2 - k_c^2)^2$, where α and k_c are material-dependent constants. Jiang *et al.* [16] reported experimental signatures of quartic dispersion in the topological insulator Sn-doped bulk $Bi_{1.1}Sb_{0.9}Te_2S$.

In this work we are going to study RKKY interactions at zero temperature for two-dimensional materials featuring quartic dispersion. We are going to calculate the Green's functions and obtain the RKKY interaction using the Green's functions. We will study the influence of the singularity in DOS on the strength, character, and amplitude of RKKY interactions. We will compare our results with the case of quadratic dispersion, where there is no singularity in the DOS.

In Sec. II we will give a a summary of the formalism for calculating exchange interaction from the Green's functions at zero temperature. In Sec. II A in particular, the already known results on two-dimensional electron systems with quadratic dispersion will be reviewed. In Sec. II B Green's functions for quartic dispersion in two dimensions will be presented and RKKY interaction will be derived and a comparison with the case of a quadratic dispersion will be presented.

II. CALCULATION OF SUSCEPTIBILITY AND THE EXCHANGE INTERACTION

The Heisenberg-type contact interaction describing the interaction between localized moments and the itinerant electron in a lattice can be written as follows:

$$V(\mathbf{r}) = \sum_{\alpha=1,2} \lambda_\alpha \mathbf{s} \cdot \mathbf{S}_\alpha \delta(\mathbf{r} - \mathbf{R}_\alpha), \tag{1}$$

*Current address: Institute for Multiscale Simulation, Friedrich-Alexander-Universität, Cauerstraße 3, 91058 Erlangen, Germany
Competence Unit for Scientific Computing, CSC, Friedrich-Alexander-Universität, Martensstraße 5a, 91058 Erlangen, Germany.
†ozgurcakir@iyte.edu.tr

where s is the spin of the itinerant electron and S_α is the impurity spin at the site $\mathbf{R}_\alpha$. $\lambda_{1,2}$ are the coupling constants. In such a system indirect exchange interactions between the impurities are mediated by the itinerant electrons and can be described by an effective Heisenberg-type spin exchange Hamiltonian

$$H' = J\,\mathbf{S}_1 \cdot \mathbf{S}_2. \tag{2}$$

Here, J is the effective coupling constant and is related to the susceptibility function as [9]

$$J = \frac{\lambda_1\lambda_2\hbar^2}{4}\chi(\mathbf{r}_1, \mathbf{r}_2). \tag{3}$$

The susceptibility function can be expressed in terms of Green's function as

$$\chi(\mathbf{r}_1, \mathbf{r}_2) = -\frac{2}{\pi}\int_{-\infty}^{E_f} \mathrm{d}E\ \mathrm{Im}\{G(\mathbf{r}_1, \mathbf{r}_2; E)G(\mathbf{r}_2, \mathbf{r}_1; E)\}, \tag{4}$$

where $\mathbf{r}_{1,2}$ denotes the position of the magnetic impurities. $G(\mathbf{r}_1, \mathbf{r}_2; E) = \langle \mathbf{r}_1|(E - \hat{H}_0 + \mathrm{i}\delta)^{-1}|\mathbf{r}_2\rangle$ is the retarded Green's function, where $\hat{H}_0$ is the Hamiltonian for the system without impurities. For a translationally invariant system, χ can be written as function of $\mathbf{R} = \mathbf{r}_1 - \mathbf{r}_2$ as follows:

$$\chi(\mathbf{R}) = -\frac{2}{\pi}\int_{-\infty}^{E_f} \mathrm{d}E\ \mathrm{Im}\{G(\mathbf{R}, E)^2\}. \tag{5}$$

A. RKKY interaction for quadratic dispersion

In this section, we will briefly review the exchange interaction for an electronic system in two dimensions with quadratic (parabolic) dispersion for comparison purposes [5].

We will consider noninteracting electrons in a two-dimensional system with low-energy excitations featuring a quadratic dispersion at the valence band edge, with an effective Hamiltonian $E(\mathbf{k}) = -\hbar^2(k_x^2 + k_y^2)/2m$. The retarded Green's function for quadratic dispersion is obtained as follows:

$$G(R; q') = -\frac{i}{4\beta}H_0^{(2)}(q'R), \tag{6}$$

where $q' = \sqrt{-E/\beta}$ with $\beta = \hbar^2/2m$ (for details see Appendix Sec. 1). Here, $H_0^{(2)}(q'R)$ is the Hankel function of the second kind. Plugging the Green's function into Eq. (5) gives the exchange energy

$$\begin{aligned} J(R) &= -\frac{\lambda_1\lambda_2\hbar^2}{16\pi\beta}\int_{k_F'}^{\infty}\mathrm{d}q'\,q' J_0(q'R)N_0(q'R) \\ &= \frac{\lambda_1\lambda_2\hbar^2 k_F'^2}{32\pi\beta}[J_1(k_F'R)N_1(k_F'R) + J_0(k_F'R)N_0(k_F'R)], \end{aligned} \tag{7}$$

where $J_n(x)$ and $N_n(x)$ are Bessel functions of the first and second kind, respectively. Here $k_\mathrm{F}' = \sqrt{-E_\mathrm{F}/\beta}$ is the Fermi wave vector. For $R \gg 1/k_\mathrm{F}'$ the exchange energy Eq. (7) shows the following asymptotic behavior [5,17–19],

$$J^{2D}(R) \simeq -\frac{\lambda_1\lambda_2\hbar^2}{16\pi}D(E_F) \times \frac{\sin(2k_F'R)}{R^2}. \tag{8}$$

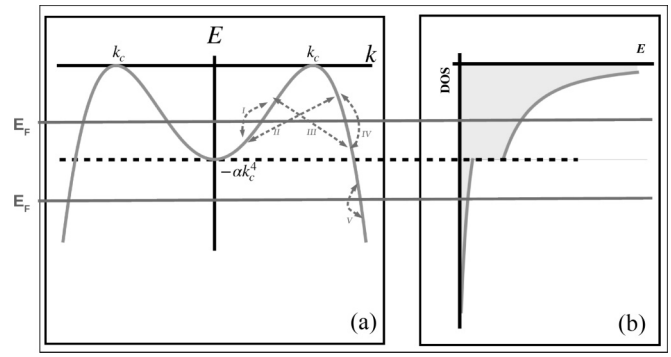

FIG. 1. (a) The Mexican-hat-type quartic dispersion, and (b) the corresponding DOS.

For the case of quadratic dispersion DOS is $D(E) = 1/(2\pi\beta)$, a constant independent of energy. At short distances, $1 \gg k_F'R$, the exchange interaction takes the form

$$J^{(2D)} \approx \frac{\lambda_1\lambda_2\hbar^2}{16\pi}k_F'^2 D(E_F)[-1.2 + 2.0\ln(k_F'R)]. \tag{9}$$

The exchange energy Eq. (7) is suppressed as $E_F \to 0$.

As a side note, RKKY interaction in doped monolayer graphene, which shows a linear dispersion, oscillates at the Fermi wavelength, with an additional spatial oscillatory factor due to intervalley scattering [6,7]. The amplitude of oscillations in doped monolayer graphene is also proportional to DOS [6].

In general, at dimensions $d = 1, 2, 3$, at long distances, $k_F'R \gg 1$, the amplitude of exchange coupling is of the form $\sim\hbar^2\lambda_1\lambda_2 D(E_F)/R^d$, oscillating as a function of distance at the Fermi wave vector $2k_F'$ [4,19].

B. RKKY interaction for quartic dispersion: Mexican-hat-type dispersion

Two-dimensional honeycomb structures with second nearest neighbor interactions may exhibit quartic dispersion at the band edge at around the Γ point. This was shown to be the case for group-VA elements [13]. Motivated by the results in Ref. [13], we will consider a Mexican-hat-type dispersion of the form

$$E = -\alpha\left(k_x^2 + k_y^2 - k_c^2\right)^2 \tag{10}$$

at the Γ point, with $\alpha > 0$. The corresponding dispersion is depicted in Fig. 1(a). In a hexagonal lattice, the system is bipartite, and the eigenfunctions come with a pseudospin term which describes the motion of the electrons in different sublattices. However, at the Γ point the system is isotropic and the electrons behave like a scalar field independent of the sublattice type. The density of states corresponding to the dispersion relation, Eq. (10), is as follows:

$$D(E) = \begin{cases} 0, & E > 0 \\ \frac{1}{2\pi\sqrt{\alpha E}}, & 0 \geqslant E \geqslant -\alpha k_c^4 \\ \frac{1}{4\pi\sqrt{\alpha E}}, & E < -\alpha k_c^4 \end{cases}, \tag{11}$$

which features a discontinuity at $E = -\alpha k_c^4$ and diverges as $\sim 1/\sqrt{E}$ as $E \to 0$ as shown in Fig. 1(b).

The retarded Green's function can be written as follows:

$$G(\mathbf{R}; E) = \frac{1}{(2\pi)^2}\int \mathrm{d}^2k \frac{e^{\mathrm{i}\mathbf{k}\cdot\mathbf{R}}}{E + \alpha\left(k_x^2 + k_y^2 - k_c^2\right)^2 + \mathrm{i}\delta}. \quad (12)$$

For $E < -\alpha k_c^4$ for a given momentum group, velocity is always in the opposite direction of the momentum, whereas for $E > -\alpha k_c^4$ there are degenerate states with group velocity either in the opposite or in the same direction as the momentum [see Fig. 1(a)]. After evaluating the integral, we obtain the Green's function as follows (see Appendix Sec. 2):

$$G(R; q) = \begin{cases} \dfrac{-1}{8\pi\alpha q^2}\left\{2K_0\left(\sqrt{q^2 - k_c^2}R\right) + i\pi H_0^{(2)}\left(\sqrt{q^2 + k_c^2}R\right)\right\}, & q^2 > k_c^2 \\ \dfrac{-i}{8\alpha q^2}\left\{H_0^{(1)}\left(\sqrt{-q^2 + k_c^2}R\right) + H_0^{(2)}\left(\sqrt{q^2 + k_c^2}R\right)\right\}, & q^2 < k_c^2 \end{cases}, \quad (13)$$

where $q = (-E/\alpha)^{1/4}$. $K_0(x)$ is the modified Bessel function of the second kind, and $H_0^{(1,2)}(x)$ are the Hankel function of first and second kind, respectively.

We will employ Eq. (3) to determine the exchange energy. For Fermi energy lying in the interval $0 > E_F > -\alpha k_c^4$ the exchange energy is as follows:

$$J(R) = \frac{\lambda_1\lambda_2\hbar^2}{\alpha}[f_1(R) + f_2(R)] \quad (14)$$

$$f_1(R) = -\frac{1}{16\pi}\int_{k_c}^{\infty} \mathrm{d}q\, \frac{1}{q}\left(N_0\left(\sqrt{q^2 + k_c^2}R\right) + \frac{2}{\pi}K_0\left(\sqrt{q^2 - k_c^2}R\right)\right)J_0\left(\sqrt{q^2 + k_c^2}R\right) \quad (15)$$

$$f_2(R) = -\frac{1}{16\pi}\int_{q_\mathrm{F}}^{k_c} \mathrm{d}q\, \frac{1}{q}\left(N_0\left(\sqrt{k_c^2 + q^2}R\right) - N_0\left(\sqrt{k_c^2 - q^2}R\right)\right)\left(J_0\left(\sqrt{k_c^2 + q^2}R\right) + J_0\left(\sqrt{k_c^2 - q^2}R\right)\right), \quad (16)$$

where $q_F = (-E_F/\alpha)^{1/4}$. The exchange energy is a function of k_cR and $q_\mathrm{F}R$.

For the case when $E_F < -\alpha k_c^4$, the exchange energy becomes

$$J(R) = -\frac{\lambda_1\lambda_2\hbar^2}{16\pi\alpha}\int_{q_\mathrm{F}}^{\infty} \mathrm{d}q\, \frac{1}{q}\left(N_0\left(\sqrt{q^2 + k_c^2}R\right) + \frac{2}{\pi}K_0\left(\sqrt{q^2 - k_c^2}R\right)\right)J_0\left(\sqrt{q^2 + k_c^2}R\right). \quad (17)$$

Here again the exchange energy is a function of k_cR and $q_\mathrm{F}R$.

At large separation when $R \gg k_\mathrm{F}^+/q_F^2$, with the Fermi wave vector given as $k_\mathrm{F}^\pm = \sqrt{k_c^2 \pm q_F^2}$, the exchange energy can be approximated as follows:

$$J(R) \simeq \frac{-\lambda_1\lambda_2\hbar^2}{8\pi}D(E_\mathrm{F}) \times \begin{cases} \frac{1}{2R^2}\left[\sin(2k_\mathrm{F}^+R) + \sin(2k_\mathrm{F}^-R) + 4\frac{\sqrt{k_\mathrm{F}^+k_\mathrm{F}^-}}{k_\mathrm{F}^+ + k_\mathrm{F}^-}\cos[(k_\mathrm{F}^+ - k_\mathrm{F}^-)R]\right], & E_\mathrm{F} > -\alpha k_c^4 \\ \frac{1}{R^2}\sin(2k_\mathrm{F}^+R), & E_\mathrm{F} < -\alpha k_c^4 \end{cases} \quad (18)$$

Here, for $E_F > -\alpha k_c^4$, there are two types of excitations with Fermi wave vectors $k_\mathrm{F}^\pm$, which produces four types of second-order processes around the Fermi level at the long-distance limit, which are schemetically shown in Fig. 1(a) with the dashed lines I–IV. For $E_F < -\alpha k_c^4$, in the long-distance limit, excitations with Fermi wave vector k_F^+ dominate, which leads to oscillations at the corresponding Fermi wave length shown in Fig. 1(a) with the dashed line V. The amplitude of RKKY interaction at the long-distance limit, Eq. (18), is proportional to the density of states at the Fermi energy.

At short distances $1 \gg k_\mathrm{F}^\pm R$, in the limits $\alpha k_c^4 \gg E_F$ and $E_F \gg \alpha k_c^4$, respectively, the exchange energy becomes

$$J(R) \simeq \frac{\lambda_1\lambda_2\hbar^2}{8\pi}D(E_\mathrm{F})q_F^2 \times \begin{cases} -4.9 + 2.0\frac{q_F^2}{k_c^2} + k_c^2R^2\left[2.0 + \frac{q_F^2}{k_c^2}(0.12 - 1.0\ln(k_cR))\right], & E_\mathrm{F} \gg -\alpha k_c^4 \\ -2.5 - 2.0\frac{k_c^2}{q_F^2} + k_c^2R^2\left[2.4 + 1.6\frac{q_F^2}{k_c^2} - \left(1 + \frac{q_F^2}{k_c^2}\right)\ln(q_FR)\right], & E_\mathrm{F} \ll -\alpha k_c^4. \end{cases} \quad (19)$$

Here in Eq. (19), the amplitude of RKKY interactions is a constant independent of Fermi energy, $\propto D(E_F)q_F^2 \propto 1/\sqrt{\alpha}$ [see Eq. (11)].

In Fig. 2, the exchange energy for $E_\mathrm{F} > -\alpha k_c^4$ in Eq. (14) is numerically computed and shown as a function of k_cR. At short range the RKKY interaction is of ferromagnetic character and there is an oscillation between ferromagnetic and antiferromagnetic character as a function of distance. As the Fermi energy gets closer to the band edge, the amplitude of the exchange energy is enhanced due to the singularity at the band edge. In the inset the long-distance behavior is shown, where a beating behavior can be seen. This behavior is

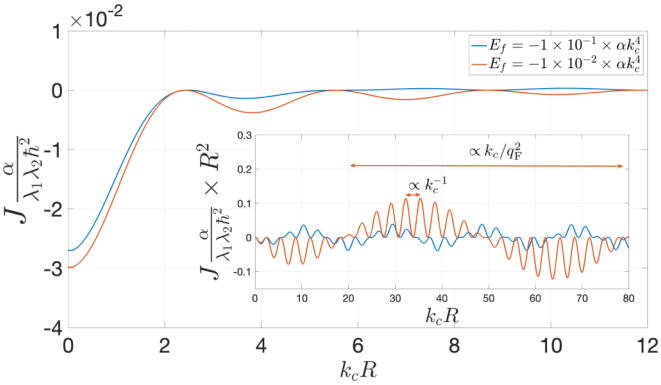

FIG. 2. Exchange energy is shown for Fermi energy $E_F > -\alpha k_c^4$, at values $E_F/(\alpha k_c^4) = -0.1, -0.01$. The inset shows the exchange energy scaled with R^2, where fast and slow oscillations have typical wavelengths π/k_c and $2\pi k_c/q_F^2$, respectively.

also evident from the long-distance behavior of the exchange energy in Eq. (18), where for $\alpha k_c^4 \gg |E_F|$ regime exchange energy behaves as

$$J \propto \frac{-1}{\sqrt{E_F}R^2} \cos\left(\frac{q_F^2}{k_c}R\right) \cos^2\left(k_cR - \frac{\pi}{4}\right), \qquad (20)$$

which is the behavior seen in the inset in Fig. 2. In Fig. 3(a) a comparison of the numerical results computed from Eq. (14) with the long-distance asymptotic behavior in Eq. (18) is presented. The exchange interactions oscillate as a function of distance and exhibit a power law decay $\sim 1/R^2$ with an amplitude $\sim 1/\sqrt{E_F}$ at large separation. It can also be seen in Fig. 2 that the RKKY interaction is of ferromagnetic character up to a distance $R \propto k_c/q_F^2$, where this region increases as $E_F \to 0$, whereas the magnitude of RKKY interactions remains finite [see Eq. (19)].

In Figs. 3(a) and 3(b) the exchange energy follows the asymptotic form in Eq. (18), which reduces to the form Eq. (20) for $\alpha k_c^4 \gg |E_F|$, exhibiting a slow oscillation at wavelength $\sim\sqrt{\alpha k_c^2/E_F} = k_c/q_F^2$ modulated by a fast oscillation at wavelength $\sim k_c^{-1}$.

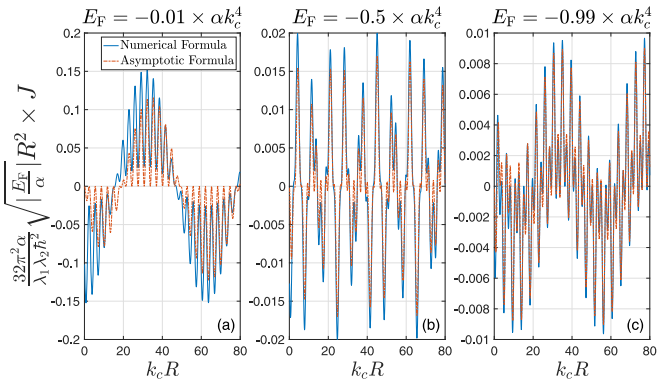

FIG. 3. Exchange energy numerically computed from Eq. (17) and its asymptotic form Eq. (18) are scaled with $\sqrt{|E_F|/\alpha}R^2$ and shown as a function of distance for Fermi energy values $E_F/(\alpha k_c^4) = -0.01, -0.5, -0.99$.

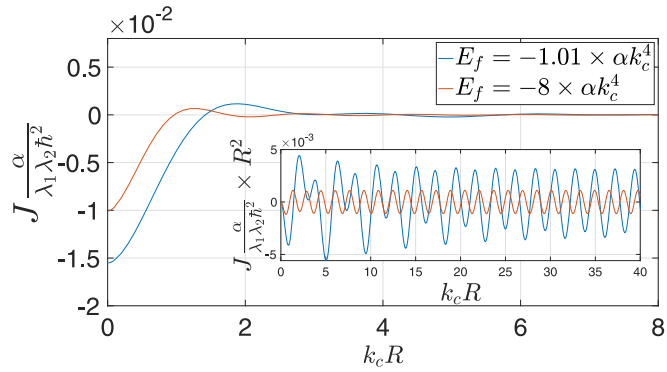

FIG. 4. Exchange energy vs distance is graphed for $E_F < -\alpha k_c^4$, at the values of Fermi energy $E_F/(\alpha k_c^4) = -1.01, -8$. In the inset the long-distance behavior is shown, where exchange energy is scaled with R^2.

For $k_F^+ \gg k_F^-$, i.e., $E_F \to -\alpha k_c^4$, the exchange energy behaves as

$$J \propto \frac{-1}{\sqrt{E_F}R^2}\left[\frac{1}{\sqrt{1+\delta^2}} \sin(2k_F^+R - \delta) + \sin(2k_F^-R)\right], \qquad (21)$$

where $\tan\delta = 4\sqrt{k_F^-/k_F^+}$. The behavior can be seen in Fig. 3(c) with fast oscillations at wavelength $\sim(k_F^+)^{-1}$ superimposed on slow oscillations at wavelength $\sim(k_F^-)^{-1}$.

In Fig. 4, exchange energy is plotted as a function of distance for $E_F < -\alpha k_c^4$. Again at short distances RKKY interaction is of ferromagnetic character and oscillates as a function of distance featuring FM/AF character. The inset in Fig. 4 shows an agreement with the asymptotic form Eq. (18), exchange energy $J \propto 1/(R^2\sqrt{E_F})$ and oscillating at the wavelength π/k_F^+.

The change in behavior of the exchange energy across $E_F = -\alpha k_c^4$ is clearly seen in Eq. (18), which can also be seen by comparing Fig. 3(c) and the inset in Fig. 4. In general there is an enhancement in RKKY interaction when the Fermi energy is above the critical value $E_F > -\alpha k_c^4$, due to an increase in DOS [see Eq. (11)].

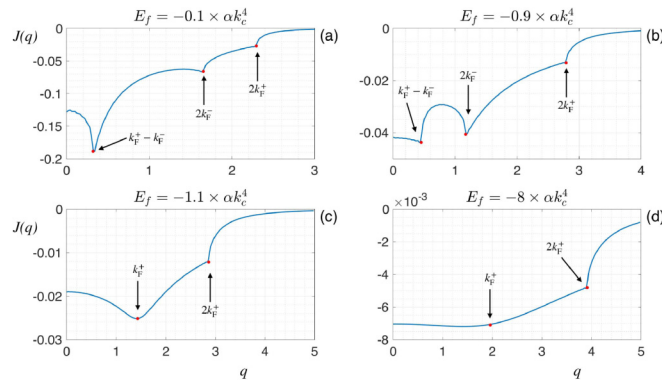

FIG. 5. Fourier transform of exchange energy $J(q)$ is shown, in units of $\lambda_1\lambda_2\hbar^2/\alpha$, as a function of q (in units of k_c) at Fermi energies $E_F/(\alpha k_c^4) = -0.1, -0.9, -1.1, -8$.

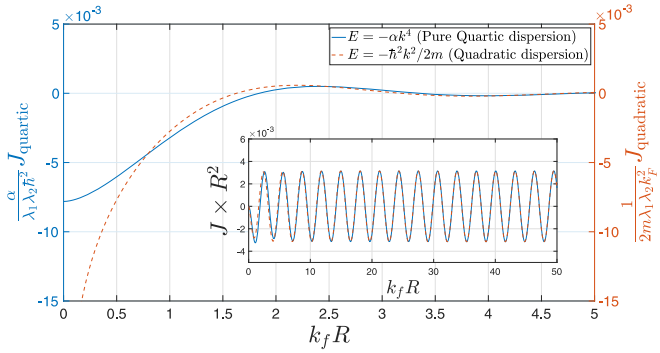

FIG. 6. Exchange energy is shown for pure quartic dispersion (blue curve) and quadratic dispersion (red curve). In the inset exchange energy scaled with R^2 is shown in units of $\lambda_1\lambda_2\hbar^2/(\alpha k_{\text{F}}^2)$ for pure quartic dispersion (blue curve) and in units of $2m\lambda_1\lambda_2$ for quadratic dispersion (red curve).

In Fig. 5, the Fourier transform of exchange energy, $J(q) = \int d^2 r J(r) e^{-i\mathbf{q}\cdot\mathbf{r}}$, is numerically computed and plotted as a function of wave vector. Figures 5(a) and 5(b) show the behavior of the susceptibility for $E_{\text{F}} > -\alpha k_c^4$. For this case, there are three values of momentum where exchange energy becomes nonanalytic, $q = 2k_{F^\pm}$ and $q = k_F^+ - k_F^-$, at which Fermi surface nesting takes place [20]. Figures 5(c) and 5(d) show the case $E_{\text{F}} < -\alpha k_c^4$, where Fermi surface nesting takes place only at $q = 2k_{\text{F}}^+$. The Fermi nesting momenta correspond to the wave vectors at which exchange energy oscillates at large distances as is seen in Eq. (18) [21].

1. RKKY interaction for quartic dispersion: Pure quartic dispersion

In the case of pure quartic dispersion $E = -\alpha(k_x^2 + k_y^2)^2$ it is sufficient to take the limit $k_c \to 0$ for the results of Mexican-hat-type dispersion with $E < -\alpha k_c^4$ in Eq. (17). This leads to the exchange energy

$$\begin{aligned} J(R) &= -\frac{\lambda_1\lambda_2\hbar^2}{16\pi\alpha}\int_{q_{\text{F}}}^{\infty} \text{d}q\, \frac{1}{q}\left(N_0(qR) + \frac{2}{\pi}K_0(qR)\right)J_0(qR) \\ &= \frac{\lambda_1\lambda_2\hbar^2}{128\pi^{\frac{5}{2}}\alpha}\left\{-G_{1,5}^{4,0}\left(\begin{matrix}1\\0,0,0,\frac{1}{2},0\end{matrix}\middle|\frac{k_F^4R^4}{64}\right)\cdots\right. \\ &\quad \left. + 4\pi G_{2,4}^{3,0}\left(\begin{matrix}\frac{1}{2},1\\0,0,0,0\end{matrix}\middle|k_F^2R^2\right)\right\}, \end{aligned} \tag{22}$$

expressed in terms of Meijer G-functions [22]. Here $k_F = (-E_{\text{F}}/\alpha)^{1/4}$ is the Fermi wave vector. The exchange energy Eq. (22), in the limits $k_F R \gg 1$ and $k_F R \ll 1$, respectively, takes the asymptotic forms

$$J(R) \simeq \lambda_1\lambda_2\hbar^2 \times \begin{cases} -D(E_{\text{F}})\dfrac{\sin(2k_F R)}{8\pi R^2}, & k_{\text{F}}R \gg 1, \\ \dfrac{-2.5 + [1.6 - \ln(k_{\text{F}}R)](k_{\text{F}}R)^2}{32\pi^2\alpha}, & k_{\text{F}}R \ll 1, \end{cases} \tag{23}$$

in agreement with the results in Eqs. (18) and (19) in $k_c \to 0$ limit. For the case of pure quartic dispersion DOS is given as $D(E) = 1/(4\pi\sqrt{\alpha E})$.

Figure 6 shows the exchange energy for pure-quartic and quadratic dispersion, Eqs. (22) and (7), as a function of distance $k_F R$. For $k_F^{-1} \gg R$, exchange energy attains a constant value for quartic dispersion independent of Fermi energy, whereas for quadratic dispersion it exhibits a logarithmic divergence, as seen in Eqs. (23) and (9). In the inset in Fig. 6, for $R \gg k_F^{-1}$, exchange energy oscillates between FM and AF character at the Fermi wavelength, featuring a power law decay $1/R^2$ for both pure quartic and quadratic dispersion, with an amplitude proportional to DOS at the Fermi energy $D(E_{\text{F}})$. This amplitude is constant for quadratic dispersion, whereas it increases as $1/\sqrt{E_{\text{F}}}$ with decreasing Fermi energy.

For pure quartic dispersion, RKKY interaction is of ferromagnetic character as $R \to 0$, and this region extends to a distance $R \propto 1/k_F$, which can be deduced from the short-distance behavior in Eq. (23). The mean value of exchange interaction within this region is a constant independent of Fermi energy,

$$\begin{aligned} \bar{J} &= \frac{1}{\pi R_0^2}\int_0^{R_0} J(R) 2\pi R dR \\ &= -\frac{\lambda_1\lambda_2\hbar^2}{\alpha} \times 0.0023, \end{aligned} \tag{24}$$

with $R_0 \simeq 1.84/k_{\text{F}}$ corresponding to the first zero of exchange energy $J(R_0) = 0$. On the other hand, the average exchange energy Eq. (24) for the quadratic case, Eq. (9), becomes proportional to the Fermi energy $\bar{J} \propto E_{\text{F}}$, which is suppressed as $E_F \to 0$.

The Fourier transform of the exchange energy Eq. (22) for pure quartic dispersion is given as follows:

$$\begin{aligned} J(\mathbf{q}) &= \int d^2 r e^{-i\mathbf{q}\cdot\mathbf{r}} J(r) \\ &= -\frac{\lambda_1\lambda_2\hbar^2}{8\pi\alpha}\left\{\frac{1}{q^2}\text{arcsinh}\left(\frac{q^2}{2k_{\text{F}}^2}\right)\cdots\right. \\ &\quad \left. + \theta(q - 2k_F)\frac{2}{q^2}\ln\left(\frac{2k_{\text{F}}}{q + \sqrt{q^2 - 4k_{\text{F}}^2}}\right)\right\}. \end{aligned} \tag{25}$$

Here the nesting takes place at $q = 2k_F$, which corresponds to the wave vector of oscillations in exchange energy at large distances [21].

For iron atoms on graphene the RKKY interaction was obtained in an *ab initio* approach [23] and with an amplitude $\propto D(E_F)/R^2$ with oscillations at the Fermi wave vector $2k_F$. The exchange coupling energy of Fe atoms to carbon atoms on graphene was at ∼2.2 eV [23]. Typically we may expect the coupling constants to be on the order of $\lambda_{1,2} \approx 1\ \text{eV} \cdot (\text{Unit Cell Area})/\hbar^2$. SnAs features a pure quartic dispersion with $k_c = 0, \alpha = 42\ \text{eV Å}^4$ [14]. From those we can expect for SnAs an RKKY coupling amplitude in Eq. (23) to be on the order of $\lambda^2\hbar^2/(8\pi^2\alpha) \approx 1\ \text{eV}/\hbar^2$.

III. CONCLUSION

We investigated RKKY-type exhange interactions for two-dimensional systems with quartic dispersion near the band edge. Quartic dispersion features a singularity in DOS at the band edge and this leads to an enhanced amplitude for

the exhange interactions at large distances, as the Fermi energy approaches the band edge. In particular for pure quartic dispersion, a region of finite magnetic exchange interaction emerges, with an average value independent of Fermi energy, up to a distance $R \approx 1/k_F$. This region increases as the Fermi energy approaches the band edge. This is in stark contrast to the case of quadratic dispersion in two dimensions where the amplitude of RKKY interaction is suppressed everywhere as the Fermi energy approaches the band edge. The materials with quartic dispersion potentially enable highly electrically/chemically tunable exchange interactions in two-dimensional systems.

ACKNOWLEDGMENT

This work has been supported by the Türkiye Bilimsel ve Teknolojik Araştırma Kurumu (TÜBİTAK) under Grant No. 115F408.

APPENDIX: GREEN'S FUNCTIONS

1. Green's function for quadratic dispersion

$$G(\mathbf{r},\mathbf{r}';E)=\frac{1}{(2\pi)^2}\int_{-\infty}^{\infty}\mathrm{d}k_x\int_{-\infty}^{\infty}\mathrm{d}k_y\frac{e^{\mathrm{i}\mathbf{k}\cdot(\mathbf{r}-\mathbf{r}')}}{E+\beta(k_x^2+k_y^2)+\mathrm{i}\delta}, \tag{A1}$$

where $\beta=\hbar^2/(2m)$.
We can write the expression as a function of $\mathbf{R}=\mathbf{r}-\mathbf{r}'$. We can choose R along the x direction without loss of generality due to the isotropy of the system [24],

$$G(R;q')=\frac{1}{(2\pi)^2\beta}\int_{-\infty}^{\infty}\mathrm{d}k_x e^{\mathrm{i}k_xR}\underbrace{\int_{-\infty}^{\infty}\frac{\mathrm{d}k_y}{k_x^2+k_y^2-q'^2+\mathrm{i}\delta}}_{I(k_x)}, \tag{A2}$$

where $q'^2=-E/\beta$. We can carry out k_y integration in Eq. (A2) in the complex plane. There are two cases where $k_x^2>q'^2$ and $k_x^2<q'^2$, and the integrand has two simple poles for each case. For $|k_x|>q$, the poles are $k_y=\pm\mathrm{i}\sqrt{k_x^2-q'^2}$, and for $|k_x|<q'$, they are given as $k_y=\pm\sqrt{q'^2-k_x^2}\mp\mathrm{i}\delta$. By carrying out the integration in Eq. (A2) in the complex plane, the integrand $I(k_x)$ can be obtained as follows:

$$I(k_x)=2\pi\mathrm{i}\left\{\frac{\theta\left(q'^2-k_x^2\right)}{-2\sqrt{q'^2-k_x^2}}+\frac{\theta\left(-q'^2+k_x^2\right)}{2i\sqrt{-q'^2+k_x^2}}\right\}. \tag{A3}$$

We can rewrite Eq. (A1) in more compact form as follows:

$$G(R;q')=\frac{1}{(4\pi)\beta}\int_{-\infty}^{\infty}\frac{e^{\mathrm{i}k_xR}}{\sqrt{k_x^2-q'^2}}\mathrm{d}k_x, \tag{A4}$$

which can be evaluated to yield

$$G(R;q')=\frac{-i}{4\beta}H_0^{(2)}(q'R). \tag{A5}$$

Here, $H_0^{(2)}(q'R)$ is the Hankel function of the second kind.

2. Green's function for quartic dispersion

The Fourier transform of Green's function can be factored as follows:

$$G(k;E)=\frac{1}{\alpha\left(k^2-k_c^2\right)^2-\alpha q^4+i\delta}, \tag{A6}$$

$$=\frac{1}{2\alpha q^2}\left(\frac{1}{k^2-k_c^2-q^2+i\delta}-\frac{1}{k^2-k_c^2+q^2-i\delta}\right), \tag{A7}$$

where $E=-\alpha q^4$.

In position space the Green's function for $E>-\alpha k_c^4$ becomes

$$G(R;q)=\frac{1}{8\alpha q^2}\left(-iH_0^{(2)}\left(\sqrt{k_c^2+q^2}R\right)-iH_0^{(1)}\left(\sqrt{k_c^2-q^2}R\right)\right). \tag{A8}$$

For $E<-\alpha k_c^4$

$$G(R;q)=\frac{1}{8\alpha q^2}\left(-iH_0^{(2)}\left(\sqrt{k_c^2+q^2}R\right)-iH_0^{(1)}\left(i\sqrt{q^2-k_c^2}R\right)\right), \tag{A9}$$

$$=\frac{1}{8\alpha q^2}\left(-iH_0^{(2)}\left(\sqrt{k_c^2+q^2}R\right)-\frac{2}{\pi}K_0\left(\sqrt{q^2-k_c^2}R\right)\right). \tag{A10}$$

[1] M. A. Ruderman and C. Kittel, Phys. Rev. **96**, 99 (1954).
[2] T. Kasuya, Prog. Theor. Phys. **16**, 45 (1956).
[3] K. Yosida, Phys. Rev. **106**, 893 (1957).
[4] Y. Yafet, Phys. Rev. B **36**, 3948 (1987).
[5] B. Fischer and M. W. Klein, Phys. Rev. B **11**, 2025 (1975).
[6] M. Sherafati and S. Satpathy, Phys. Rev. B **84**, 125416 (2011).
[7] E. Kogan, Graphene **02**, 8 (2013).
[8] S. Saremi, Phys. Rev. B **76**, 184430 (2007).
[9] M. Sherafati and S. Satpathy, Phys. Rev. B **83**, 165425 (2011).
[10] N. Klier, S. Shallcross, and O. Pankratov, Phys. Rev. B **90**, 245118 (2014).
[11] N. Klier, S. Sharma, O. Pankratov, and S. Shallcross, Phys. Rev. B **94**, 205436 (2016).
[12] A. U. Canbolat and O. Çakır, Phys. Rev. B **100**, 014440 (2019).
[13] H. Sevinçli, Nano Lett. **17**, 2589 (2017).
[14] B. Özdamar, G. Özbal, M. N. Çınar, K. Sevim, G. Kurt, B. Kaya, and H. Sevinçli, Phys. Rev. B **98**, 045431 (2018).
[15] M. N. Çınar, G. O. Sargın, K. Sevim, B. Özdamar, G. Kurt, and H. Sevinçli, Phys. Rev. B **103**, 165422 (2021).
[16] W. Jiang, B. Li, X. Wang, G. Chen, T. Chen, Y. Xiang, W. Xie, Y. Dai, X. Zhu, H. Yang, J. Sun, and H.-H. Wen, Phys. Rev. B **101**, 121115(R) (2020).
[17] C. Kittel, in *Indirect Exchange Interactions in Metals*, edited by F. Seitz, D. Turnbull, and H. Ehrenreich, Solid State Physics Vol. 22 (Academic Press, New York, 1969), pp. 1–26.

[18] M. T. Béal-Monod, Phys. Rev. B **36**, 8835 (1987).
[19] V. I. Litvinov and V. K. Dugaev, Phys. Rev. B **58**, 3584 (1998).
[20] W. Kohn, Phys. Rev. Lett. **2**, 393 (1959).
[21] D. N. Aristov and S. V. Maleyev, Phys. Rev. B **56**, 8841 (1997).
[22] Y. L. Luke, *The Special Functions and Their Approximations* (Academic Press, New York, 1969).
[23] Y. Zhu, Y. F. Pan, Z. Q. Yang, X. Y. Wei, J. Hu, Y. P. Feng, H. Zhang, and R. Q. Wu, J. Phys. Chem. C **123**, 4441 (2019).
[24] R. T. Couto, Rev. Brasil. Ensino Fís. **35**, 01 (2013).